J Mol Model (2010) 16:737–748
DOI 10.1007/s00894-009-0558-2

ORIGINAL PAPER

Topological analysis of aromatic halogen/hydrogen bonds by electron charge density and electrostatic potentials

Darío J. R. Duarte · Margarita M. de las Vallejos · Nélida M. Peruchena

Received: 5 March 2009 / Accepted: 5 May 2009 / Published online: 10 October 2009

Abstract In this work, the intermolecular distribution of the electronic charge density in the aromatic hydrogen/halogen bonds is studied within the framework of the atoms in molecules (AIM) theory and the molecular electrostatic potentials (MEP) analysis. The study is carried out in nine complexes formed between benzene and simple lineal molecules, where hydrogen, fluorine and chlorine atoms act as bridge atoms. All the results are obtained at MP2 level theory using cc-pVTZ basis set. Attention is focused on topological features observed at the intermolecular region such as bond, ring and cage critical points of the electron density, as well as the bond path, the gradient of the density maps, molecular graphs and interatomic surfaces. The strength of the interaction increases in the following order: F···π < Cl···π < H···π. Our results show that the fluorine atom has the capability to interact with the π–cloud to form an aromatic halogen bond, as long as the donor group is highly electron withdrawing. The Laplacian topology allows us to state that the halogen atoms can act as nucleophiles as well as electrophiles, showing clearly their dual character.

D. J. R. Duarte · M. M. de las Vallejos · N. M. Peruchena
Departamento de Química, Laboratorio de Estructura Molecular y Propiedades, Área de Química Física, Facultad de Ciencias Exactas y Naturales y Agrimensura,
Universidad Nacional del Nordeste,
Avda. Libertad 5460,
3400 Corrientes, Argentina

N. M. Peruchena (✉)
Facultad Regional Resistencia,
Universidad Tecnológica Nacional,
French 414,
3500 Resistencia, Chaco, Argentina
e-mail: arabeshai@yahoo.com.ar

Keywords AIM · Charge density · Halogen bond · Laplacian · Molecular electrostatic potentials

Introduction

In the broad field of weak interactions, the hydrogen bond HB, and in particular the aromatic hydrogen bond aHB, (where a π–electron system acts as a proton acceptor), have been the object of several experimental and theoretical investigations. Still today the interest on this topic is in steady growth [1-4]. At present, it has been noted a renewed interest in the halogen bonding XB [5, 6], an attractive noncovalent interaction that can play a significant factor in biological recognition processes similar to hydrogen bonding.

In the XB, a halogen atom is shared between an atom, a group or a molecule that "donates" the halogen and another that "accepts" it. In other words, a halogen atom X is shared between a donor D and an acceptor A. In halogen bonding, (like hydrogen bonding) the donor tends to be electron-withdrawing, with high electronegativity and the acceptor is usually a Lewis base, with at least an available pair of electrons [7]. However, a π–electron system can also act as a hydrogen acceptor (*i.e.*, in aromatic hydrogen bonds) and numerous examples have been discussed in the bibliography. In this respect, we think that a π–electron system can act as a halogen acceptor and this fact should be investigated and should be take into account in the drug design.

Generally the XBs are weaker than the HBs, but some exceptions have been found in which the binding energy of the former is higher than the latter. In a recent paper Regier Voth et al. have demonstrated that a halogen bond formed between a brominated uracil and phosphate oxygen can be

engineered to direct the conformation of a biological molecule. This has revealed that, when a Br···O interaction is placed in direct competition against a classic HB, the bromine interaction is estimated to be approximately 2–5 kcal mol^{-1} stronger than the analogous hydrogen bond [8]. Politzer et al. have compared the computed interaction energies and vibrational frequency shifts associated with the formation of a series of halogen-bonded and hydrogen-bonded complexes. They found that the hydrogen bond is usually the stronger one, although there are exceptions, as in the case of bromine [9]. Furthermore Sandorfy et al. have shown via infrared spectra that the XB can compete and interfere with the HB [10-13]. It is not surprising that the hydrogen (with partial positive charges) interacts attractively with electronegative atoms (such as N, O, S, F, Cl, etc.) but why do halogen atoms, (with partial negative charges) show a behavior similar to hydrogen and can be attracted by other atoms with available lone pair? Recently, Politzer et al. [14] have responded to this question, by means of an examination of the molecular electrostatic potential maps in compounds containing covalently−bonded halogen atoms, D–X. They found that the halogen atom X (Cl, Br and I) has a small region (cap) of positive electrostatic potential on its outermost portions, centered along the extension of the D–X bond. In consequence, they have attributed the formation of a halogen bond to the attractive electrostatic interaction between the cap of positive electrostatic potential (in the bridge halogen atom) and a lone pair of the acceptor atom. A recent study on interactions involving ammonia and halofluoromethanes has shown that the binding energies of $CF_3X\cdots NH_3$ increase from 2.0 to 6.0 kcal mol^{-1} moving along the series X = Cl, Br, I, and the progressive introduction of fluorine atoms in methyl-iodides raises the interaction energy from 3.0 kcal mol^{-1} for CH_3I to 6.0 kcal mol^{-1} for CF_3I [15]. It is clear that the XBs shows similar characteristics to the ones of the hydrogen bond in strength and directionality [5]. However, XB is more directional than HB. Afterward, it is well established that halogen bonding increases in strength in the order Cl < Br < I [14]. Unlike the other halogen atoms, the fluorine atom is frequently said not to form halogen bonds; although a study recently carried out has provided theoretical evidence that the fluorine atom covalently linked to R group, has the capability to form XB, if R is a suitable electron withdrawing group [14]. Then, in FCN molecule the -CN group is sufficiently electron withdrawing to create a positive electrostatic potential on the fluorine atom (in their axial region). This fact suggests that the participation of the fluorine atom in the formation of the halogen bond is feasible, as well as in the aromatic halogen bond [16]. For this reason, we devoted special attention to $NCF\cdots\pi C_6H_6$ system in this work. A detailed understanding of the physical origin and scope of hydrogen bonding and halogen bonding interactions has become an important goal of physical organic chemistry. These interactions play a dominant role in many forefront areas of modern chemistry, and are now being exploited to control the assembly of small molecules in the design of supramolecular complexes and new materials [17-20]. In addition, it has also been proposed that aromatic halogen bonding could play an important role in the crystal structures of proteins. Then, a crystallographic study was also undertaken to investigate the role of C–X···π interactions (with X = F, Cl, Br, I) in organic compounds [21] and in protein structures [22]. Unexpectedly, the results show that the propensity for the formation of C–X···π interactions is higher in case of fluorine atoms than in other halogens [21, 22].

According to our knowledge, and in contrast with the large number of experimental and theoretical investigations aimed to deepen the understanding of the aHB interactions, the aXB interactions have received less attention especially from the theoretical point of view. As a consequence, there is a vast sea of open questions about the aXB interaction nature. In previous works, we have analyzed the topology of the charge density distribution in other weak and moderate interactions produced in several chemistry fields [23-26]. Recently we also have investigated the change produced -on the molecular structure and the biological properties- by the substitution of hydrogen by fluorine atoms in a sexual pheromone of insect [27]. This study was undertaken with the purpose to understand the loss of biological activity in halogenated analogues in relation to the molecular recognition processes -by the linking of pheromone and halogenated analogues to pheromone binding protein, (PBP). In this work, in order to gain insight into the nature of these interactions and their potential effects, we carried out a local topological properties analysis of the electronic charge density distribution within the framework of the atoms in molecules (AIM) theory [28] and a study of the electrostatic interactions through the molecular electrostatic potential (MEP) maps, as well [29]. Nine simple complexes ($D–Y\cdots\pi C_6H_6$, with Y = H, F, Cl) were selected (see Scheme 1). The selected hydrogen/halogen donor molecules exhibit strong withdrawing effects on the bridge atom (*i.e.*, D = -F, -CN). Also, the hydrogen substituent (*i.e.*, D = -H) of insignificant effect was used for comparison (as blank).

The main purpose of the present work is to provide an answer to the following questions:

1. Can a fluorine atom participate in aromatic halogen bonds? In what situations can a fluorine atom be expected to participate in aromatic halogen bonds?
2. Is the strength of the aXBs comparable to the one of aHBs?

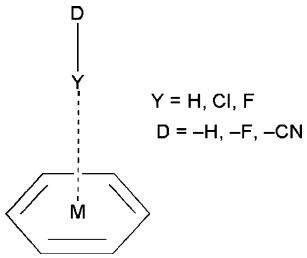

Scheme 1 Schematic diagram of the aH-bonded and aX-bonded complexes, both in form of T-shape. M represents the ring midpoint

3. Are the topological features of the T-shape aXBs similar to the ones of aHBs?
4. Can an analysis based on the electron charge density and its Laplacian contribute to understanding the nature of the aromatic halogen bonds?

Finally, one of the key reasons for studying the strength and topological characteristic of aXBs is to acquire understanding of the contribution that these types of interactions can make to protein-ligand interactions, which might be important in many fields within biological and ecological chemistry as well as within medicinal chemistry.

Methods and calculation details

The geometries of all the monomers and complexes were optimized without any constraint, using the second order Møller–Plesset perturbation method (MP2) [30], which is acceptable to an accurate description of noncovalent interaction, such as aHBs and aXBs [31-35]. In addition, it is now well established that diffuse and polarization functions must be included in the basis set in order to adequately describe the non spherical atomic density and polarizability effect. Thus, all calculations were performed with the correlation-consistent basis set of Dunning, conventionally denoted cc–pVTZ [36]. We employed a T−shape configuration in which, the donor D–H and D–X groups are oriented along the normal line to the benzene plane passing through the ring center as the starting geometry for D–H···πC_6H_6 and D–X···πC_6H_6 complexes.

The binding energies (ΔE) of each complex were calculated as the difference between the total energy of the complex and the sum of total energies of the two monomers isolated. The basis set superposition error (BSSE) was taken into account using the counterpoise method proposed by Boys and Bernardi [37].

The calculations of local topological properties of the electron charge density at critical point, as well as, the display molecular graphs were performed with the AIM2000 package [38], with the wave functions obtained at MP2/6–311++G** level.

Electrostatic potential surfaces were generated by mapping the electrostatic potentials onto surfaces of constant molecular electron density (0.001 au in Fig. 4 and 0.01 au in Fig. 5). The figures of the molecular electrostatic potential (MEP) maps were created with the Molekel program [39, 40]. All calculations were carried out using the Gaussian 03 suite of programs [41].

Results

In the present study we have evaluated nine complexes, as shown in Scheme 1. The donor molecules: ClCN and FCN were chosen following Politzer et al. work [16], who had already calculated their MEPs. In addition, the HCN donor molecule was included for a comparison between them. The aH–bonded complexes NCH···πC_6H_6, and FH···πC_6H_6 have been previously studied from a theoretical point of view [42].

In our study, we considered as donor molecules the F–Y and the NC–Y and we also added the H–Y molecule (where the bridge atom (Y) is bonded to the smaller non–electron withdrawing group).

Geometrical and energetic parameters

In this work, the T–shape configuration of the complexes was taken into account (Scheme 1). All monomers and complexes were fully optimized during the calculations to MP2 level using cc–pVTZ basis set. For Y = H, highly symmetric configurations were obtained (*i.e.*, D–H perpendicular to benzene molecule). All the geometric structures of the aH–bonded complexes were confirmed as true minima by a vibrational analysis. In the case of aX–bonded complexes, two degenerate low imaginary frequencies were found (These frequencies are associated with the swinging vibrational motion of the lineal molecule over the aromatic ring). In all cases, these complexes are useful to carry out a comparative analysis between both types of interactions to T–shape configuration.

Table 1 reports the selected optimized geometrical parameters, along with the variations in the bond donor distance upon complexation Δd(D–Y), that is, the difference between the distance d(D–Y) in the complexes and in the isolated monomers. MP2 results, obtained with a cc-pVTZ basis set, for binding energy without (ΔE) and with BSSE correction (ΔE^{corr}) are also given in Table 1.

As can be seen in Table 1, through the binding energy analysis, all these complexes (with the exclusion of the H–F···πC_6H_6 complex) are being stabilized as a consequence of the interaction between the hydrogen/halogen atom and the π–electron of the benzene. It should be pointed out that, for the first time, we are giving evidence of the formation of

Table 1 Calculated structural parameters and variations in the donor bond distance d(D–Y) upon complexation. The binding energies of the complexes without (ΔE) and with correction are also given (ΔE^{corr}) [a]

Complexes	$d(Y\cdots C\pi)^b$	$d(Y\cdots M)^c$	Δd(D–Y)	ΔE	BSSE	ΔE^{corr}
$HF\cdots\pi C_6H_6$	3.5562	3.2658	−0.0004	0.08	0.65	0.74
$FF\cdots\pi C_6H_6$	3.3225	3.0160	0.0034	−1.52	0.64	−0.89
$NCF\cdots\pi C_6H_6$	3.3213	3.0146	−0.0022	−1.99	0.61	−1.38
$HCl\cdots\pi C_6H_6$	3.6554	3.3793	0.0009	−1.71	0.45	−1.26
$FCl\cdots\pi C_6H_6$	3.4831	3.1918	0.0061	−3.72	0.86	−2.86
$NCCl\cdots\pi C_6H_6$	3.4938	3.2035	−0.0004	−4.00	0.61	−3.39
$HH\cdots\pi C_6H_6$	3.0835	2.7506	−0.5311	−1.14	0.25	−0.89
$FH\cdots\pi C_6H_6$	2.5866	2.1784	−0.3467	−5.33	1.62	−3.72
$NCH\cdots\pi C_6H_6$	2.6502	2.2535	−0.2156	−5.31	0.74	−4.57

[a] Energies in kcal mol^{-1} and distances in angstroms (Å). [b] Correspond to the distance between the Y atom and each of carbon atom of the benzene molecule. [c] Correspond to the distance between the Y atom and benzene molecule midpoint. [d] In all cases the value of the D–Y···M angle is 180°

stable complexes that involves the D–F···π interaction. The binding energy values show that the aHB interactions are relatively stronger than the aXB interactions and increases in the order $D–F\cdots\pi C_6H_6$ < $D–Cl\cdots\pi C_6H_6$ < $D–H\cdots\pi C_6H_6$. As was previously indicated, the $H–F\cdots\pi C_6H_6$ complex gives a positive ΔE value when the BSSE correction is included, which indicates its instability. The binding energies calculated at the MP2/cc–pVTZ level lie between −3.39 to −1.26 kcal mol^{-1} for $D–Cl\cdots\pi C_6H_6$ complexes and are even lower (−0.89 and −1.38 kcal mol^{-1}) for $F–F\cdots\pi C_6H_6$ and $NC–F\cdots\pi C_6H_6$ complexes respectively. However, their values are comparable in strength with the reported values for other conventional H···ππ interactions considered "weak hydrogen bonds" by Gravowski [43] (*i.e.*, −1.43 kcal mol^{-1} for $C_2H_2\cdots\pi C_2H_2$ in T–shape complex at MP2/6–311++G(2df,pd) level. In consequence, the aromatic halogen bond can be considered a "weak bond" (near to 4.0 kcal mol^{-1}). However, when the chlorine atom is the "bridge atom" an increase in the strength of the aXB is observed. It is important to emphasize that in the $NCCl\cdots\pi C_6H_6$ complex, the electronic binding energy was found to be only 26% weaker than in the $NCH\cdots\pi C_6H_6$ complex. However, a notable decrease is observed in the binding energy for the $NCF\cdots\pi C_6H_6$ complex (around of 60% weaker that the Cl···π interaction). In addition, it is well established that, the strength of the halogen bond interaction increases simultaneously with the increase in size of the halogen, that is, with the van der Waals radii (r_{vdw}) (r_{vdw} Cl= 1.75 Å y r_{vdw} F=1.35 Å) [44]. Notice that the polarizability increases in the same way [45, 46]. In accordance to the previous observation, the results show that the $D–F\cdots\pi C_6H_6$ complexes, even though weak, are still formed. Previously, it has been proposed that, the fluorine atom has nothing or little possibility to form halogen bonds. In addition, the interactions where the π-system acts as a proton acceptor are considered as a weak acceptor [2]. Therefore, the stability of the $NCF\cdots\pi C_6H_6$ and $FF\cdots\pi C_6H_6$ complexes is an interesting and novel fact. We believe, like Politzer [14], that the stable character of the interactions (D–F···π) involving fluorine atoms, is due to the electron withdrawing effect of the donor groups on them.

The cyano group displays the behavior of the stronger electron withdrawing group and, in accordance to what is expected in the aromatic hydrogen/halogen bonds, the binding energy increases following the order $NC–F\cdots\pi C_6H_6$ < $NC–Cl\cdots\pi C_6H_6$ < $NC–H\cdots\pi C_6H_6$. As a comparison, the strength of the aromatic chlorine bond decreases in the order $NC–Cl\cdots\pi C_6H_6$ > $F–Cl\cdots\pi C_6H_6$ > $H–Cl\cdots\pi C_6H_6$ (*i.e.*; ΔE^{corr} = −3.39; −2.86 and −1.26 kcal mol^{-1}, respectively). The decrease in strength when the chlorine atom is bonded to cyano group in the $NC–Cl\cdots\pi C_6H_6$ complex, in relation to the chlorine atom bonded to the F atom in the $F–Cl\cdots\pi C_6H_6$ complex is 16% and the decrease in strength between this last one and the $H–Cl\cdots\pi C_6H_6$ complex is 56%.

In contrast, when the fluorine atom is the engaged atom, the binding energy in $NC–F\cdots\pi C_6H_6$ is 35% higher than in $F–F\cdots\pi C_6H_6$. Additionally, when D = H, a stable complex will not be form. The F–H and NC–H molecules at the front to bases such as NH_3 and H_2O [47] show that the strength of the interaction in $FH\cdots OH_2$ is 38% higher than in $NCH\cdots OH_2$ and that $FH\cdots NH_3$ is 52% higher that $NCH\cdots NH_3$. These results are interesting because the situation is different in the cases we studied here. We have found that the decrease of the strength between $NC–X\cdots\pi C_6H_6$ and $F–X\cdots\pi C_6H_6$ complexes is 16 % when the chlorine atom is the bridged atom and it is higher (35%) when fluorine is the bridged atom.

From the data in Table 1, it can be seen that, the intermolecular distances $d(Y\cdots C\pi)$ and the distances

between the Y atom and the M, d(Y···M), in aH-bonded complexes are shorter than in the aX-bonded complexes. In the formers, the distances d(H···C_π) and d(H···M), span a range between 2.6502–3.0835 Å and 2.2535–2.7506 Å, respectively. These values are in agreement with the proposed range for weak interactions as C–H···π, where the d(H···C_π) distance varies from 2.0 to 3.0 Å [2]. In the same sense, the distances d(Cl···C_π) and d(F···C_π) vary from 3.4831 to 3.6554 Å and from 3.3213 to 3.3225 Å respectively, which are in agreement with the experimental range of X···π bond distances (average value of 3.525± 0.007 Å for Cl···π and 3.224±0.025 Å for F···π) [21]. Furthermore, and in particular, the data calculated for the NCH···πC_6H_6 and FH···πC_6H_6 complexes show similar characteristics with those obtained by other authors [42]. Different behaviors are shown by the D–Y donor bonds, corresponding to the different types of interactions upon the complexation. In the aHBs, D–Y bond lengths increase (Δd (D–Y) = from −0.5311 in H-H···πC_6H_6 to −0.2156 Å in NC-H···πC_6H_6). In contrast, the D–X bond lengths in the aX-bonded complexes, show an increase only when the cyano group is the halogen donor. In the other cases the length of the halogen donor bond is slowly shortening. It should be clarified that upon complexation only very little changes are observed for the geometries of the aromatic systems. (Data not shown).

Local topological properties

The topological analysis of the electron density constitutes a powerful tool to investigate the electronic properties of the molecular system and allows a deep examination of the interatomic interactions. In addition, this methodology has been successfully applied in the study of the properties of a variety of conventional and unconventional hydrogen bond [3, 28, 48] as well as of the halogen bond [49]. The aromatic hydrogen/halogen complexes studied here comprise a combination of three moieties: -CN, -F, -H with hydrogen, fluorine and chlorine as bridged atoms and the benzene molecule. Six bond paths (BP, lines of atomic interactions of maximum electronic density) connect the hydrogen/halogen bridged atom (Y = H, F, and Cl) of the donor molecule, with each carbon atom of the benzene molecule, (Y···Cπ). On these BPs, six bond critical points (BCP) or (3, −1) critical points are found and six (3, +1) ring critical points (RCPs), and one (3, −3) cage critical point (CCP) are located in the intermolecular regions in all π–complexes studied here. The topological features of these complexes are displayed in Fig. 1 and Table 2.

Table 2 reports the calculated local topological properties at the BCPs, at the RCPs and at the CCP of the complexes studied here. As was previously indicated, the H–F···πC_6H_6 complex is unstable (gives a positive ΔE^{corr} value) and, in consequence, is not included. In addition, the electron densities, ρ, and the Laplacian, $\nabla^2\rho$, are given for all these points. The values of ellipticity, ε, the relationship $|\lambda_1|/\lambda_3$ and the relationship between the energetic properties, such as local kinetic energy density, G, and local potential energy density, $|V|$, at critical points, CPs, are also included. Calculated properties at the BCP are labeled with the subscript "b" throughout the work.

The eight stable π−complexes show a similar topological pattern (only three molecular graphs are shown in Fig. 1). The two unique trajectories, that originate at the BCP and terminate at each of the neighboring nuclei, define a line along which the hydrogen/halogen atom is engauged to each carbon atom in the benzene molecule, where the electron charge density is a maximum with respect to any neighboring line. These are "seven-center" interactions, where the bridge atom is engauged to each carbon atom in the benzene molecule. Due to this fact, the topological properties at each BCP show low values of electron charge density and Laplacian. The charge density values lie in the order of 0.0047 to 0.0059 au. and of 0.0053 to 0.0087 au. for aXBs and aHBs, respectively. The Laplacian values in all complexes are positive and are the result of the interaction between two closed-shell systems. It should be clarified that the topological pattern displayed at the bond paths of the complexes involved in the D–F···π interaction (Fig. 1b), presents similar characteristics to those of the D–H···π interaction (Fig. 1a); as it is shown in Fig. 1. Similar patterns of topology have been found in several aH-bonded complexes, (for example the FH···πC_6H_6, the HCCH···πC_6H_6, etc.), [31, 42] as well as in complexes that involved cation/π interactions, (for example (Li^+, Na^+, K^+)···πC_6H_6) [50]. All the complexes studied here show the characteristic of being highly symmetric structures. It is important to note that the six Cl···Cπ bond paths are curved closed to the chlorine atom. This is due to the greater electronic charge density concentration in the equatorial region in relation to the axial region of the chlorine atom. The asymmetry in the distribution is more noticeable in chlorine atoms that in fluorine atoms in D–X dador molecules. In addition, we should expect that this effect will be even greater in bromine and iodine atoms due to their bigger size and polarizability.

As was previously expressed, we have found that the values of the charge density (and its principal axes of curvature) at the intermolecular BCPs, in the complexes analyzed here, are relatively low, (within the range of 4.8×10^{-3} to 8.2×10^{-3} au.). However, the decrease of ρ_b values is a characteristics of bifurcated hydrogen/halogen bonds (or three center interactions) [51] as well as of other complexes linked by multiple bond path (*i.e.*, T–shape complexes or multicenter interactions). Still, they are bigger than that reported for other unconventional X–H···π/σ

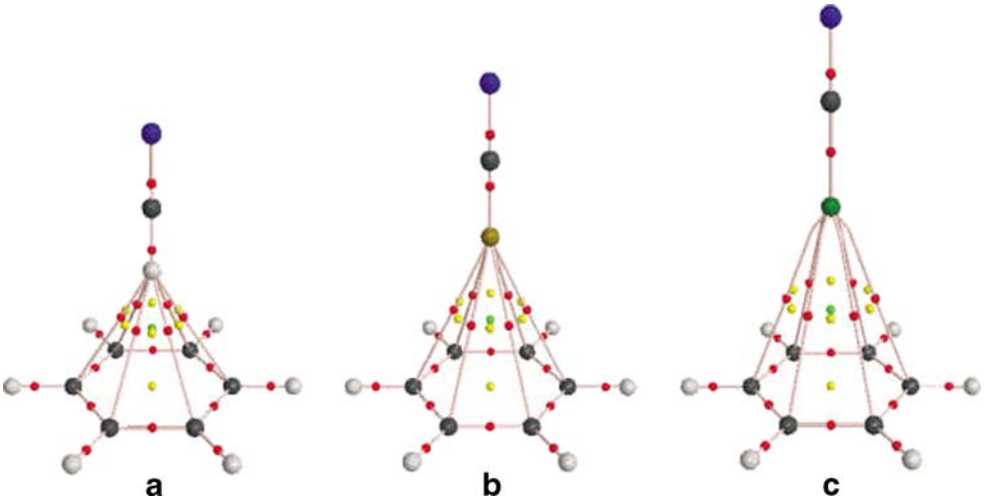

Fig. 1 Molecular graphs for (**a**) NCH···πC_6H_6, (**b**) NCF···πC_6H_6 and (**c**) NCCl···πC_6H_6 complexes. The lines connecting the nuclei are the bond paths. Red dots and yellow dots represent BCPs (3, −1) and RCPs (3, +1), respectively. The position of the CCP, (3, +3) is indicated with a green dot

interactions (*i.e.*, 3.3×10^{-3} au. for $C_2H_2\cdots H_2$ σ–complex and 7.7×10^{-3} au. for $C_2H_2\cdots C_2H_2$ π-complex) recently considered by Gravowsky as hydrogen bonds [43]. Accompanying the lower ρ_b value; as was expressed before, a positive $\nabla^2\rho_b$ value is observed in aromatic hydrogen and halogen bond, Y···Cπ. In addition, the relationship between the perpendicular and parallel curvature at BCP, $|\lambda_1|/\lambda_3$, and the relationship between the potential and kinetic density energies, $|V_b|/G_b$ are always less than one. This indicator reveals that the kinetic energy contribution is greater than that of the potential energy at the BCP, and shows depletion of the electronic charge along the bond path. Nevertheless, the intermolecular BCPs display the hallmarks of "closed−shell" interactions.

Figure 2 shows the electron density contour maps and the gradient vector fields of ρ(r), with the superposition of the molecular graph and interatomic surfaces, in the plane containing all atoms from a donor molecule and two

Table 2 Local topological properties of the electron charge density at the bond, ring, and cage critical points in the intermolecular region, in the studied complexes

Complexes	CP	ρ	$\nabla^2\rho$	ε	$\lvert\lambda_1\rvert/\lambda_3$	$\lvert V\rvert/G$
FF···πC_6H_6	Y···Cπ	0.0050	0.0205	18.1099	0.1323	0.8168
	(3, +1)	0.0050	0.0205	22.3973	0.1352	0.8134
	(3, +3)	0.0039	0.0201	0.0005	0.2340	0.8013
NCF···πC_6H_6	Y···Cπ	0.0049	0.0207	19.5487	0.1274	0.8045
	(3, +1)	0.0049	0.0207	21.9540	0.1302	0.8014
	(3, +3)	0.0039	0.0206	0.0000	0.2277	0.7929
HCl···πC_6H_6	Y···Cπ	0.0047	0.0166	15.4457	0.1250	0.7397
	(3, +1)	0.0047	0.0166	20.3436	0.1282	0.7372
	(3, +3)	0.0037	0.0166	0.0000	0.2414	0.7682
FCl···πC_6H_6	Y···Cπ	0.0057	0.0203	16.8364	0.1321	0.7493
	(3, +1)	0.0057	0.0203	16.3407	0.1358	0.7455
	(3, +3)	0.0044	0.0197	0.0001	0.2708	0.7738
NCCl···πC_6H_6	Y···Cπ	0.0059	0.0216	14.2151	0.1287	0.7448
	(3, +1)	0.0059	0.0216	16.5432	0.1325	0.7404
	(3, +3)	0.0045	0.0210	0.0000	0.2710	0.7650
HH···πC_6H_6	Y···Cπ	0.0053	0.0167	40.7144	0.1485	0.8220
	(3, +1)	0.0053	0.0168	31.1718	0.1508	0.8206
	(3, +3)	0.0047	0.0184	0.0003	0.2672	0.8280
FH···πC_6H_6	Y···Cπ	0.0074	0.0265	27.6596	0.1492	0.7550
	(3, +1)	0.0074	0.0265	30.2964	0.1520	0.7524
	(3, +3)	0.0064	0.0259	0.0000	0.3013	0.7708
NCH···πC_6H_6	Y···Cπ	0.0087	0.0300	23.4331	0.1586	0.7876
	(3, +1)	0.0087	0.0300	26.0535	0.1621	0.7841
	(3, +3)	0.0073	0.0311	0.0000	0.3815	0.8028

[a] ρ and $\nabla^2\rho$ are in ua. and ε, $|\lambda_1|/\lambda_3$ and $|V|/G$ are dimensionles. [b] The BCPs (3, −1), and the RCPs (3, +1) correspond to six critical points equal by symmetry. The symbols are explained in the text.

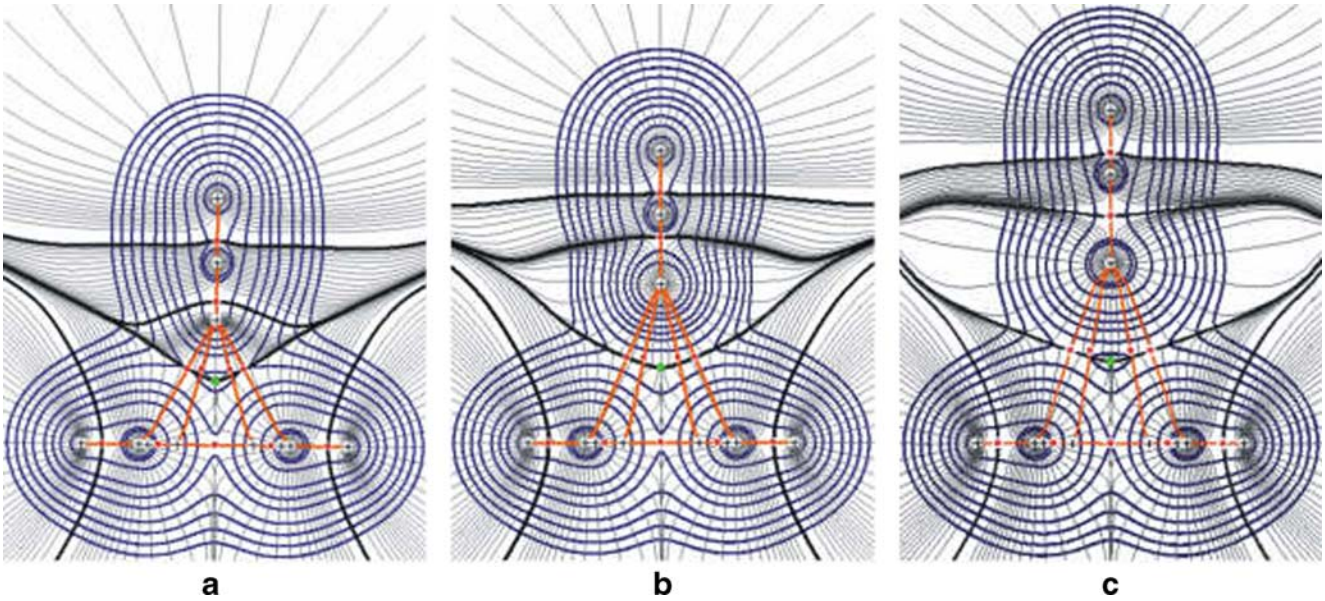

Fig. 2 A representations of the gradient vector field of ρ(r) overlaid with the contour plots of ρ(r) for the complexes (**a**) NCH···πC$_6$H$_6$, (**b**) NCF···πC$_6$H$_6$, and (**c**) NCCl···πC$_6$H$_6$. In each case the plane illustrated contains two carbon nuclei (and two hydrogen) of the benzene molecule (π–electron donor) and all the nuclei of the D–Y molecule. In the displays of the gradient vector fields the set of trajectories (gray lines) which terminate at a given nucleus or attractor (cross) defines the basin of that attractor. The pair of trajectories which, in this plane, terminate at each bond critical point (3, −1) (red dot) mark the intersection of an interatomic surface (black lines) with the plane of the figure. The trajectories, which originate at the bond critical points and define the bond paths, are shown in orange lines. In addition, the cage critical point (3, +3) is indicated by a green dot. The trajectories associated with the bond critical points define the boundaries of the atoms and the molecular graph. In the contour plots of ρ(r) (indicated with blue lines), the outer line equals 0.001 au and the remaining contour lines increase in value in the order 2×10n, 4×10n, and 8×10n, with n=−3, −2, −1

extreme C–H bonds of the benzene molecule (T-shape) for the (a) NCH···πC$_6$H$_6$, (b) NCF···πC$_6$H$_6$ and (c) NCCl···πC$_6$H$_6$ complexes. Lu et al. [32], have found higher density values in the F–Cl···C$_6$H$_5$–X (with X = -H, -NO$_2$, -CN, -Br, -Cl, -F, -CH$_3$, -OH, and -NH$_2$) systems at the intermolecular Cl···π BCP than those reported in this paper. In Lu's work, the topological pattern is different because the chlorine atom interacts with two adjacent carbon atoms of the aromatic molecule. Anyhow, the aXBs show lower charge density values at the X···Cπ BCP in relation with the conventional XB (*i.e.*, FCl···NH$_3$) [49]. In the aHBs, the density values at the intermolecular BCP show an accordance with the values obtained by other authors.

In all cases, these intermolecular BCPs lie very close to the RCPs, which shares, essentially, the same value of ρ_b. There is a nearly flat bottom surface in the distribution of the electron density linking these BCPs and RCPs. The penetration of the bridged atom localized at the D–Y molecule on the electronic density of the π–electron donor systems can be clearly observed in the map of the gradient trajectories of ρ(r) (see Fig. 2). As expected, it is found that the values of charge density at the BCP between each pair of bonded atoms increases with their mutual penetration [52].

Finally, the set of complexes analyzed here allows us to draw an idea about the behavior of the halogen atom in the near space to an aromatic ring. Thus, we consider evident that the formation of an aromatic halogen bond should be expected. Subsequently, this leads us to believe that the formation of an aromatic halogen bond should be considered in ligand-protein complexes.

On the other hand, the topological description of the Laplacian of the electronic density distribution, $\nabla^2\rho_b$, is a powerful tool in the interpretation of quantum chemical results. It provides an enhanced view of the local form of the electronic density. We believe that a deep knowledge of the asymmetrical distribution of the charge density (axial and equatorial regions) around the halogen atoms is essential in order to understand the electron redistribution mechanisms that occur during the attractive interaction between the halogen atom and the π-clouds. For this reason, we describe, in the following sub-section, a study based on the topology of the Laplacian.

Laplacian topology of the charge density

More accurately than the topology of the ρ, the topology of the Laplacian of the charge density can show, in a tridimensional chart, whether the charge density is either maximally concentrated or maximally depleted. In the first case, (maximally concentrated) it is possible to report which sites are able to deliver electronic charge and, in

consequence, if they are especially reactive toward electron-poor reactants (such as hydrogen atoms involved in hydrogen bonds). In the second case, it is possible to show which sites are able to stabilize an overloaded uptake of electronic charge and if they are especially reactive toward electron-rich reactants (*i.e.*, electronegative atoms or π-electron).

The Laplacian function of an atomic system exhibits a shell of charge concentration and a shell of charge depletion for each quantum shell. In accordance with other authors [53, 54] it is convenient, for a more intuitive interpretation, to consider the $-\nabla^2\rho$ function for our studies. A (3, −3) CP corresponds to a local maximum in $-\nabla^2\rho$ (with $\nabla^2\rho<0$), and indicates a local electronic charge concentration (CC), while a (3, +3) CP corresponds to a local minimum in $-\nabla^2\rho$, (with $\nabla^2\rho>0$) and indicates a local depletion of the electronic charge (CD). The outer quantum shell of an atom over $\nabla^2\rho<0$ is called valence shell charge concentration (VSCC) [53]. For an isolated atom, a sphere is located where the valence electronic charge is maximally and uniformly concentrated. However, the VS loses its uniformity when the atom is involved within a chemical bond. In consequence, the electron charge density distributions on their surfaces (and the resulting electrostatic potentials) are not uniform. It is important to highlight that the distribution of the charge density at the VS of an atom in a molecule is non-uniform, even if the Laplacian is all positive (charge depletion zone at the VS) or all negative (charge concentration zone at the VS). For example, in the Laplacian topology, the non bonded maxima of VSCC or (3,−3) nb-CP (generally associate with lone pairs in oxygen, nitrogen and halogen atoms) are connected (between each other) by a link critical point or (3,−1) CP denoted by *l*-CP at VSCC. This link point indicates that the charge concentration is a maximum in both perpendicular directions to the path that connects two local maxima in the charge concentration and a minimum along this line. The analysis of maxima and link points serves to characterize the distortion of the VSCC of the chlorine atom by the formation of the F-Cl bond. In the same sense, in the region of the charge depletion, or VSDC, a (3, +1) CP is a minimum of charge concentration in two of the three directions of the space.

The surface of $-\nabla^2\rho=0$ has been used as an indicator of chemical reactivity for organic molecules [28]. Thus, we have used the distribution of the Laplacian function for the localization of the preferential sites of attack between the nucleophiles and the electrophiles in the complexes we studied here. Figure 3 summarizes the results for the F-Cl···πC_6H_6 complex. The most heavily shaded regions represent the area of charge concentration, where the VSCC is the outer one. Also, Fig. 3a shows the (3, −3) critical points in $-\nabla^2\rho$, or CC maxima points on the molecular graph (networks of bond path in the density topology). These points show the localizations (in the plane of the figure) of bonded and non-bonded maxima for the F-Cl···πC_6H_6 complex. In addition, the minimum point (or charge depletion point) in the VSCD of the halogen atom is shown. In the F-Cl molecule the chlorine atom bonded to a more electronegative atom, shows an asymmetrical distribution of the electron charge density on its reactive surface. Considering the molecular plane of the halogen donor molecule, to the right and to left of the F-Cl bond direction, it is evident that the equatorial region is rich in electrons (and a charge concentration zone is observed). In contraposition, the axial region along the F-Cl bond is reduced or poor in electrons (and a zone of depletion of charge density is observed in this direction). It is important to emphasize that the existence of nonbonding maxima in the VSCC of the chlorine atom, indicates the sites for an electrophilic attract and in the same sense the minima of CC in the VSCD indicates the sites for a nucleophilic attract [28, 55-59]. Therefore, it is evident that those atoms with (3, +1) CPs in their valences shell are candidate for such a type of attack. The existence of this last point on the chlorine atom in the F-Cl bond is indicative of an electrophilic site or, in other words, of a local deficiency in electrons.

In Fig. 3a, we can see that the chlorine atom exhibits a great region of charge depletion in its VS. Subsequently, the chlorine atom in the F-Cl···πC_6H_6 complex showed an increased capability for a nucleophilic attack because it has a greater region of charge depletion to be filled by the electron density provided by a nucleophile. This same feature is clearly display at the envelope graph (Fig. 3b) where a hole on the reactive surface of the chlorine atom at the halogen donor bond is shown. These results are consistent with Politzer's observation about the existence of the σ-hole, defined as "a decrease of the electronic population along the D-X direction".

We have found that in the D–X halogen donor molecules, the equatorial region at the halogen atoms is a site that exhibits the highest concentration of charge. In contraposition, the axial region along the D–X direction is a site of charge depletion. In consequence, the Laplacian topology clearly shows that the chlorine, and even the fluorine, can undergo a stabilizing interaction with electrophiles (oriented in equatorial direction) as well as with nucleophiles in axial orientation.

Politzer et al. have reported that "the chlorine (as well as bromines and iodines) atoms have the rather surprising feature of a region of positive electrostatic potential on the outermost portion of their surface, centered around the extension of the R–X bond". In the same sense, our work shows that the chlorine atom, in the halogen donor bond site (F–Cl compound), has a region of depletion of charge density on the outermost portion of its reactive surface which is also centered around the extension of the D–X

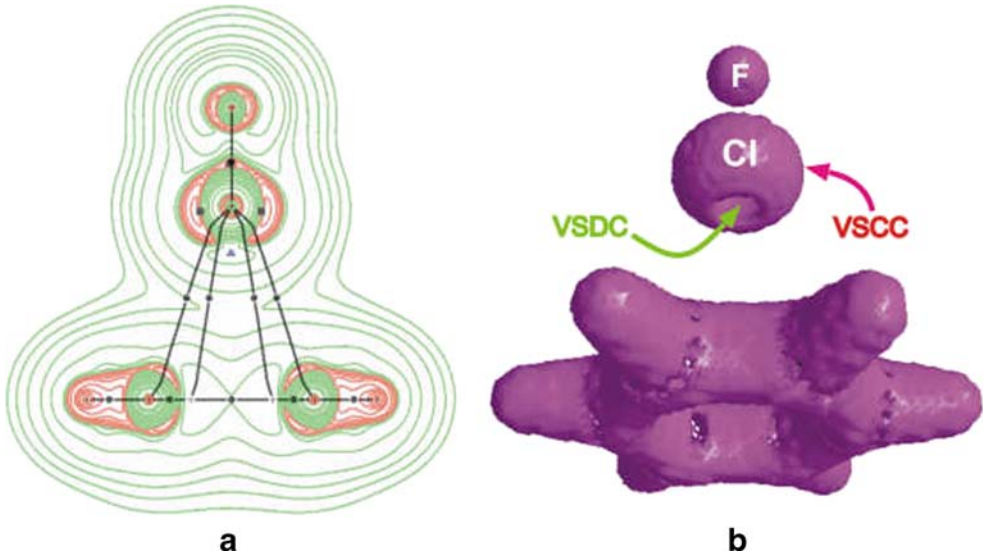

Fig. 3 (**a**) Contour map of the $-\nabla^2\rho(r)$ distribution and molecular graph for the FCl···πC_6H_6 complex, in the plane that contains the chlorine and the fluorine atoms and two C−H bonds of the benzene (the benzene molecule is localized in a plane perpendicular to the previous one). Lines connecting the nuclei are the bond paths and the small dots along them represent the bond critical point (BCP). Dark lines (red in the version online) represent regions of electronic charge concentration, and gray lines (green in the version online) denote regions of electronic charge depletion. The contours of the $\nabla^2\rho$ (r) increase (+)/decrease (−), respectively, from the zero contour in the order $\pm2\times10^{-n},\pm4\times10^{-n},\pm8\times10^{-n}$, with n beginning at 3 and decreasing in steps of unity. The molecular graph is superimposed. (**b**) Surface of $\nabla^2\rho=0$, for FCl···πC_6H_6 complex (envelope in $\nabla^2\rho=0$)

bond. Such depletion is less evident, but not absent, in others chlorine donor bonds (*i.e.*, H–Cl and NC–Cl compounds, results not shown).

In summary, all complexes studied here show a (3, +1) CP in the direction of D–Y bond and opposite to D, in other words a local depletion of charge density in D–Y···πC_6H_6 complexes is observed at all times. In consequence, the dual character, as a nucleophile as well as an electrophile, of the halogen atoms is well decrypted by the Laplacian of the electronic charge density topology. In consequence, in halogen bonds "halogens attract halogens", as well as in aromatic halogen bonds "halogens attract π-electrons". Furthermore, it is important to mention here that the halogen acceptor capacity (in the scarce set analyzed here) might be affected by the substitution of hydrogen atoms by active groups on the benzene molecule.

Molecular electrostatic potentials maps

The electrostatic potential V(r) that is created at a point r by a nucleus of the molecule and electrons can be calculated through the next equation:

$$V(r) = \sum_A \frac{Z_A}{|R_A - r|} - \int \frac{\rho(r')dr'}{|r' - r|}$$

in which Z_A is the charge on nucleus A, located at R_A, and ρ(r) is the electronic density function of the molecule. The first term is the contribution from the atomic nuclei and the second term is the contribution electronic to the electrostatic potential.

The MEP formalism allows the rigorous calculation of the electrostatic interaction between any classical charge and the undisturbed molecule, without considering the induction, dispersion, and repulsion effects [60, 61].

To analyze the electrostatic behavior of the axial antibonding D–Y in the considered molecules, we computed the V(r) at MP2/6–311++G** level. We have considered the isosurfaces of the electronic equivalent to ρ(r)=0.001 au. This contour of the molecular electronic density, represents the effective molecular volume.

Figure 4 shows the three-dimensional MEP maps of the (a) FCN, (b) ClCN, and (c) HCN molecules in au. The regions of the map range from red (−0.027 au, more negative zone) through green to blue (+0.044 au., more positive zone). From a simple visual analysis of the electrostatic potential surfaces, it is observed in the most outer region of the bridge atoms (H, F, and Cl) that there is a depletion of the electron charge density (potential values more positive, "cap", on hydrogen and chlorine atoms and less negative on fluorine atom). The intensity of this depletion follows this order H > Cl > F. This tendency is in accordance with what is reported in the bibliography [28]. Furthermore, these results are in correlation with the binding energy that we present in Table 1. In contraposition, it should be noted that, in the MEP maps of the D–Y compounds, where D = -CN, -F and -H, with the same Y atoms the correlation with the binding energy is not

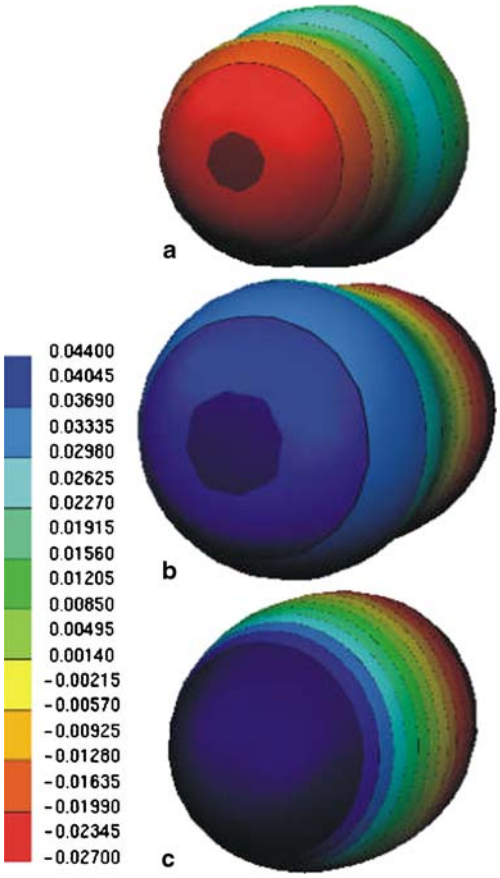

Fig. 4 Molecular electrostatic potential (MEP) of (**a**) FCN, (**b**) ClCN, and (**c**) HCN molecules, mapped on the surface of molecular electron density 0.001 au). The values of the MEP varies between −0.027 (red) and +0.044 (blue) au

observed. In Fig. 5 the MEP maps of the NCCl···πC_6H_6 complex, and the isolated benzene molecule are displayed at the same scale.

We can observe that the size of the negative electrostatic potential regions decreases on the π-cloud, upon the complexation. In addition, the electrostatic potential on hydrogen atoms of the benzene molecule, take more positive values. All these observations suggest that electrostatic energy plays a fundamental role in both interactions (aHB and aXB). The decrease or depletion of the electronic density on the most outer region (head) of hydrogen/halogen atoms, which make them more prone to take up the charge density provided by π-cloud, cause an electronic displacement in the benzene molecule, directed to the center of the aromatic ring.

Conclusions

This work supports the formation of D-Cl···π and again D–F···π interactions in NCF···πC_6H_6 and FF···πC_6H_6 complexes. It is in accordance to the original proposal of Politzer et al. (based in MEP's analysis) which states that even fluorine atoms can form halogen bonds.

The formation of the studied complexes results from the interaction between the charge density provided by the π-cloud (benzene molecule) and the charge density depletion region localized at the outest region of the halogen or hydrogen atoms in the direction of the D-(X, H) bonds. Such charge density depletion, on the halogen/hydrogen atoms, results from the electron density withdrawing from the tail of the donor molecule

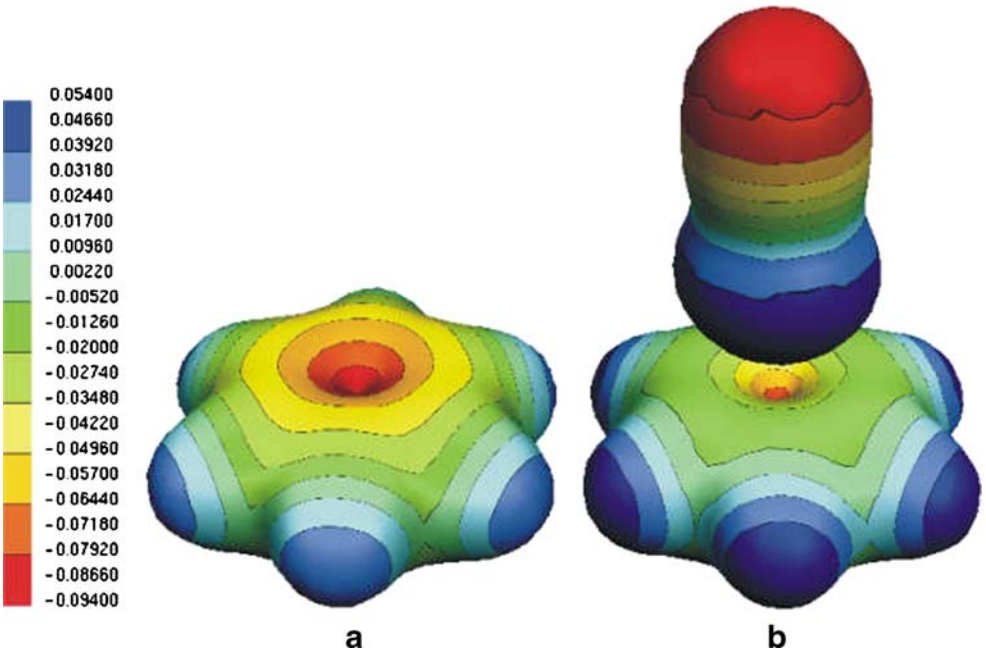

Fig. 5 Molecular electrostatic potential (MEP) of (**a**) benzene molecule and (**b**) NCCl···πC_6H_6 complex, mapped on the surface of molecular electron density (0.01 au). The values of the MEPs varies between −0.094 (red) and +0.054 (blue) au

(*i.e.*, cyano group). This generates a decrease of the charge density in the head of the donor molecule (halogen/hydrogen atom), which makes these atoms more prone to uptake the charge density provided by π−cloud of the benzene molecule.

Although the X···π interactions in the aXBs are weaker than the H···π interactions in the aHBs, both are a consequence of the same facts described in the previous paragraph. These facts can be appropriately characterized by the topology of the charge density distribution.

This study demonstrates that both AIM and MEP analysis are valuable complementary tools to elucidate the nature of intermolecular interactions in aHB and aXB. The topology of the distribution of the Laplacian of the electronic density allowed us to state that halogen atoms can act as nucleophiles as well as electrophiles, showing, clearly, their dual character. From a topological view point, the extremes or critical points in the distribution of the Laplacian easily provide the precise localization of different reactivity zones. Finally, it is worth stressing that this conclusion is based on a real physical property of the system: the electron charge density that can be obtained experimentally or by computational methods. Indeed, it is important to consider (in contraposition to the electrostatic potentials) that the AIM formalism proposed by Bader is very consistent and physically supported because the electronic density is pondered while the quantum-mechanical observable. In addition, it is interesting to highlight that, (and opposite to previous published studies about halogen bridged compounds), an exploration on the Laplacian has not been done yet.

The present results suggest that the quantification of the depletion of the charge density in halogen atoms in a more extended set of complexes is necessary. This is under investigation in our laboratory and results will be published in the near future.

To conclude, our results demonstrated that the aromatic halogen bonds could be significant in the design of novel drugs or bioactive molecules (for example, fluorinated analogues of pheromones with grater stability in field tests). What is more, the admittance that these interactions (XBs and aXBs) are stable and can help us to think how the drug action at the binding site of the receptors may occur.

Acknowledgments The authors acknowledge financial support from SECYT - UNNE (Secretaría de Ciencia y Tecnología - Universidad Nacional del Nordeste), PICTO (Proyecto de Investigación Científica y Tecnológica Orientado) 089. Margarita de las Mercedes Vallejos and Darío Jorge Roberto Duarte are fellows of SECYT- UNNE. Nélida Maria Peruchena is a career researcher of CONICET (Consejo Nacional de Investigaciones Científicas y Técnicas), Argentine.

References

1. Nishio M, Hirota M, Umezawa Y (1998) The CH/π interaction. Wiley, New York
2. Desiraju RG, Steiner T (1999) The weak hydrogen bonding structural chemistry and biology. Oxford University Press, Oxford
3. Hobza P, Havlas Z (2000) Chem Rev 100:4253–4264
4. Ran J, Wong MW (2006) J Phys Chem A 110:9702–9709
5. Bent HA (1968) Chem Rev 68:587–648
6. Hassel O (1970) Science 170:497–502
7. Politzer P, Lane P, Concha MC, Ma Y, Murray JS (2007) J Mol Mod 13:305–311
8. Regier Voth A, Hays FA, Shing Ho P (2007) Proc Nat Acad Sci USA 104:3971–3978
9. Politzer P, Murray JS, Lane P (2007) Int J Quantum Chem 107:3046–3052
10. Bernard-Houplain MC, Sandorfy C (1973) Can J Chem 51:1075–1082
11. Bernard-Houplain MC, Sandorfy C (1973) Can J Chem 51:3640–3646
12. Di Paolo T, Sandorfy C (1974) Chem Phys Lett 26:466–469
13. Di Paolo T, Sandorfy C (1974) Can J Chem 52:3612–3622
14. Clark T, Hennemann M, Murray JS, Politzer P (2007) J Mol Mod 13:291–296
15. Valerio G, Raos G, Meille SV, Metrangolo P, Resnati G (2000) J Phys Chem A 104:1617–1620
16. Politzer P, Murray JS, Concha MC (2007) J Mol Mod 13:643–650
17. Nishio M (2004) Cryst Eng Commun 6:130–158
18. MacGillivray LR, Holman KT, Atwood JL (2001) J Supramol Chem 1:125–130
19. Metrangolo P, Neukirch H, Pilati T, Resnati G (2005) Acc Chem Res 38:386–395
20. Auffinger P, Hays FA, Westhof E, Shing Ho P (2004) Proc Nat Acad Sci 101:16789–16794
21. Prasanna MD, Row TNG (2000) Cryst Eng 3:135–154
22. Saraogi I, Vijay VG, Das S, Sekar K, Row TNG (2003) Cryst Eng 6:69–77
23. Sosa GL, Peruchena NM, Contreras RH, Castro EA (2002) THEOCHEM 577:219–228
24. Fidanza NG, Survire F, Lobayan R, Sosa GL, Enriz RD, Peruchena NM (2001) THEOCHEM 543:185–193
25. Masman MF, Zamora MA, Rodriguez AM, Fidanza NG, Peruchena NM, Enriz RD, Csizmadia IG (2002) Eur Phys J D 20:531–542
26. Fidanza NG, Sosa GL, Lobayan R, Peruchena NM (2005) THEOCHEM 722:65–78
27. Chamorro E, Sequeira A, Zalazar MF, Peruchena NM (2008) J Bioorg Med Chem 16:8535–8545
28. Bader RFW (1990) Atoms in molecules. A quantum theory. Clarendon Press, Oxford Science
29. Scrocco E, Tomasi J (1973) Top Curr Chem 42:95–170
30. Møller C, Plesset MS (1934) Phys Rev 46:618–622
31. Novoa JJ, Mota F (2000) Chem Phys Lett 318:345–354
32. Lu Y-X, Zou J-W, Wand Y-H, Yu Q-S (2007) Int J Quantum Chem 107:1479–1486
33. Van Mourik T, Price SL, Clary DC (2000) Chem Phys Lett 331:253–261
34. Tarakeshwar P, Choi HS, Kim KS (2001) J Am Chem Soc 123:3323–3331
35. Van Mourik T (2004) Chem Phys 304:317–319
36. Jensen F (1999) Introduction to computational chemistry. Wiley, New York, USA
37. Boys SF, Bernardi F (1970) Mol Phys 19:553–566
38. Blieger-König F, Schönbohn J (2000) AIM2000 Program Package, Version 2.0 Copyright 2002, Chemical adviser by Bader

RFW, Büro fur Innovative Software Strieibel Blieger-König, Germany
39. Flükiger PF (1992) Development of the molecular graphics package MOLEKEL and its application to selected problems in organic and organometallic chemistry. Thèse No. 2561. Département de chimie physique, Université de Genève, Genève
40. Portmann S, Lüthi HP (2000) CHIMIA 54:766–770 http://www.cscs.ch/molekel/index.html
41. Frisch MJ, Trucks GW, Schlegel HB, Scuseria GE, Robb MA, Cheeseman JR, Montgomery JA Jr, Vreven T, Kudin KN, Burant JC, Millam JM, Iyengar SS, Tomasi J, Barone V, Mennucci B, Cossi M, Scalmani G, Rega N, Petersson GA, Nakatsuji H, Hada M, Ehara M, Toyota K, Fukuda R, Hasegawa J, Ishida M, Nakajima T, Honda Y, Kitao O, Nakai H, Klene M, Li X, Knox JE, Hratchian HP, Cross JB, Adamo C, Jaramillo J, Gomperts R, Stratmann RE, Yazyev O, Austin AJ, Cammi R, Pomelli C, Ochterski JW, Ayala PY, Morokuma K, Voth GA, Salvador P, Dannenberg JJ, Zakrzewski G, Dapprich S, Daniels AD, Strain MC, Farkas O, Malick DK, Rabuck AD, Raghavachari K, Foresman JB, Ortiz JV, Cui Q, Baboul AG, Clifford S, Cioslowski J, Stefanov BB, Liu G, Liashenko A, Piskorz P, Komaromi I, Martin RL, Fox DJ, Keith T, Al-Laham MA, Peng CY, Nanayakkara A, Challacombe M, Gill PMW, Johnson B, Chen W, Wong MW, Gonzalez C, Pople JA (2004) Gaussian 03, Revision D.01. Gaussian, Inc, Wallingford, CT
42. Cubero E, Orozco M, Hobza P, Luque FJ (1999) J Phys Chem A 103:6394–6401
43. Grabowski SJ (2007) J Phys Chem A 111:3387–3393
44. Bondi A (1964) J Phys Chem 68:441–451
45. Metrangolo P, Resnati G (2008) Halogen bonding. Fundamnetals and applications. Springer, Berlin
46. Metrangolo P, Pilati T, Resnati G (2006) Cryst Eng Comm 8:946–947
47. Oliveira BG, Pereira FS, de Araujo RCMU, Ramos MN (2006) Chem Phys Lett 427:181–184
48. Koch U, Popelier PLA (1995) J Phys Chem 99:9747–9754
49. Lu Y-X, Zou J-W, Wand Y-H, Yu Q-S (2006) THEOCHEM 776:83–87
50. Mohajeri A, Karimi E (2006) THEOCHEM 74:1–6
51. Lu Y-X, Zou J-W, Wand Y-H, Yu Q-S (2006) THEOCHEM 767:139–142
52. Carroll MT, Bader RFW (1988) Mol Phys 65:695–722
53. Popelier PLA (2000) Coord Chem Rev 197:169–189 and references therein
54. Lobayan RM, Sosa GL, Jubert AH, Peruchena NM (2004) J Phys Chem A 108:4347–4356
55. Popelier P (2000) Atoms in molecules, an introduction, Prentice Hall, Manchester
56. Bader RFW, Chang C (1989) J Phys Chem 93:2946–2956
57. Carroll MT, Cheseeman JR, Osman R, Weinstein H (1989) J Phys Chem 93:5120–5123
58. Carroll MT, Chang C, Bader RFW (1988) Mol Phys 63:387–405
59. Murgich J, Franco HJ, San-Blas G (2006) J Phys Chen A 110:10106–10115
60. Stewart RF (1972) J Chem Phys 57:1664–1668
61. Naray-Szabo G, Ferenczy GG (1995) Chem Rev 95:829–847